Calcein labelling and electrophysiology: insights on coral tissue permeability and calcification

Eric Tambutté[1], Sylvie Tambutté[1,*], Natacha Segonds[1],
Didier Zoccola[1], Alexander Venn[1], Jonathan Erez[2,†]
and Denis Allemand[1,†]

[1]*Centre Scientifique de Monaco, Avenue Saint Martin 98000, Monaco*
[2]*Institute of Earth Sciences, The Hebrew University of Jerusalem, Edmond Safra Campus,
Jerusalem 91904, Israel*

The mechanisms behind the transfer of molecules from the surrounding sea water to the site of coral calcification are not well understood, but are critical for understanding how coral reefs are formed. We conducted experiments with the fluorescent dye calcein, which binds to calcium and is incorporated into growing calcium carbonate crystals, to determine the permeability properties of coral cells and tissues to this molecule, and to determine how it is incorporated into the coral skeleton. We also compared rates of calcein incorporation with rates of calcification measured by the alkalinity anomaly technique. Finally, by an electrophysiological approach, we investigated the electrical resistance of coral tissues in order to better understand the role of tissues in ionic permeability. Our results show that (i) calcein passes through coral tissues by a paracellular pathway, (ii) intercellular junctions control and restrict the diffusion of molecules, (iii) intercellular junctions should have pores of a size higher than 13 Å and lower than 20 nm, and (iv) the resistance of the tissues owing to paracellular junctions has a value of 477 ± 21 Ohm cm^2. We discuss the implication of our results for the transport of calcium involved in the calcification process.

Keywords: coral; biomineralization; membrane permeability; calcium transport; cell junctions; para/transcellular transport

1. INTRODUCTION

The calcification of corals underpins the largest biomineralized structures on the planet: coral reefs. Coral skeletons themselves are widely used to infer past environmental conditions in the Earth's history. However, despite an abundant literature on coral calcification (for reviews see [1–8]), mechanistic aspects of this process still remain enigmatic, especially the mechanisms behind the transport of calcium at the level of the calcifying cells (i.e. the calicoblastic cells; for reviews see [1,9]). Indeed, three potential pathways have been proposed: (i) an active transcellular transport of calcium through calicoblastic cells, (ii) a passive paracellular diffusion of calcium or sea water between calicoblastic cells, and (iii) a combination of transcellular and paracellular pathways.

The data in favour of an active transcellular pathway rely on physiological experiments [10–12] that have produced kinetic and pharmacological data, which show that inhibitors of transcellular calcium carriers also inhibit calcification. Moreover, data obtained from molecular approaches show the presence of a calcium channel [13] and a CaATPase [14] in calicoblastic cells that could be responsible for a transcellular transport of

calcium. However, these data are not conclusive since many epithelial cells (even in non-calcifying organisms) contain similar carriers and to date no functional analysis has been conducted to establish their role in calcification. Furthermore, pharmacological inhibitors may not be specific to calcium transport for calcification but also to calcium carriers involved in other processes of cell physiology, such as regulation of endocytotic and exocytotic pathways, and can therefore indirectly affect coral calcification.

Arguments in favour of a passive paracellular pathway in corals—in which bulk sea water (external unmodified) arrives at the site of calcification, where its composition can be modified by enzymes—have been presented by several authors [14,15–18]. One important source of data supporting the existence of a paracellular pathway arises from experiments that show cell impermeant molecules such as calcein or alizarine (which are used to stain coral skeletons during calcification) are incorporated into the skeletons [3,15,17–20], suggesting that these molecules follow a paracellular pathway. These observations are puzzling when considered against histological data, where paracellular pathways are usually distinguished from transcellular pathways based on the morpho-functional properties of intercellular epithelial junctions. In corals, based on ultrastructural studies, septate junctions have been described between calicoblastic cells [7,21,22]. These junctions are usually considered in invertebrates as the counterparts of tight junctions in

vertebrates, which constitute barriers to the paracellular transport of ions [23]. However, in a freshwater mollusc, it has been shown that these junctions are permeable to calcium (with at least 50 per cent of transport being paracellular [24]) and thus one can question their role in coral tissue permeability.

The aim of the current study was to investigate the variable lines of evidence obtained on the pathway of ions/molecules with respect to their implication for coral calcification. We thus conducted experiments with calcein to determine the permeability properties of coral cells and tissues to the molecule and to determine how it is incorporated into coral skeleton. We also compared rates of calcein incorporation with rates of calcification measured by the alkalinity anomaly technique. Finally, by an electrophysiological approach, we looked at the electrical resistance of coral tissues in order to better understand the role of tissues in ionic permeability.

2. MATERIAL AND METHODS

(a) *Biological material*
The majority of the experiments were performed on the scleractinian coral *Stylophora pistillata*, and some experiments were performed on the Mediterranean sea anemone *Anemonia viridis*; both were maintained in the laboratory in controlled conditions of culture (see the electronic supplementary material). Coral apexes were cut into small fragments to obtain microcolonies cultivated on nylon nets [25] or grown on glass coverslips or glass slides [22,25–28]. For experiments, all incubations of living specimen were performed under the same environmental conditions of light intensity, pH and temperature as in culture conditions.

(b) *Calcein experiments*
Calcein is a fluorescent label that binds to calcium and is incorporated into growing calcium carbonate crystals [29]. Calcein was purchased from Sigma-Aldrich. A concentrated solution containing $2 \, \mathrm{g \, l^{-1}}$ calcein was prepared in distilled water and buffered to pH 6 with sodium bicarbonate to enhance solubility [29]. This concentrate was then diluted in filtered sea water (fSW; pore size filter $= 0.2 \, \mu m$) buffered at pH 8.2 with NaOH to obtain a final concentration ranging between 0 to $160 \, \mu M$ (fSW-calcein), depending on the experiment.

(c) *Preparation of samples for calcein experiments*
(i) *Qualitative measurements of calcein incorporated into calcium carbonate*
To investigate the incorporation of calcein into skeletons or inorganic calcium carbonate crystals, samples were incubated for 20 min with fSW-calcein $20 \, \mu M$. Observations were performed with a fluorescent macroscope and spectra were obtained with a spectrofluorimeter (see below).

(ii) *Quantitative measurements of calcein incorporated into calcium carbonate*
To measure both calcein incorporation into the skeleton and calcification, microcolonies prepared as described above were incubated for 2, 4, 6 and 24 h in fSW-calcein $20 \, \mu M$. Half of the samples were used for calcification measurements by the alkalinity anomaly technique [30] and half of the samples were used to determine calcein incorporated into the skeleton. For calcein incorporation, tissues were removed

by the treatment with NaOCl 10 per cent in distilled water for 30 min and then skeletons were rinsed three times in distilled water and dried at room temperature. Skeletons were then dissolved with HCl 2N and the solution was neutralized with NaOH to pH 8.2.

A standard curve of calcein at concentrations varying from 0.05 to $20 \, \mu M$ in fSW was prepared in the same conditions as the samples (HCl treatment and NaOH neutralization, pH 8.2) and was used as a calibration curve to determine the quantity of calcein incorporated into the coral skeletons. Measurements of calcein were obtained with the confocal system (see below), by spectral analysis with excitation at 488 nm. The correlation coefficient of the calibration curve of calcein was 0.9914.

(iii) *Permeability of tissues to calcein*
To determine if calcein passes through a paracellular or a transcellular pathway, live microcolonies grown on glass coverslips were incubated for 20 min in 5 ml of fSW-containing calcein in fSW (concentration specified for each experiment). Observations were performed with the confocal microscope (see below).

More details on sample preparation are given in the electronic supplementary material.

(d) *Fluorescent beads experiments*
Red fluorescent Fluospheres (carboxylate-modified microspherical beads of 20 nm, 200 nm and $2 \, \mu m$ were purchased from Molecular Probes (ref. F8887).

To determine if fluorescent beads were incorporated into the skeleton, microcolonies were incubated for 24 h (12 L : 12 D cycle) in 50 ml fSW-containing 2 per cent fluorescent beads (each size independently) under mixing with a magnetic stirrer. Samples were then rinsed for 10 min in 25 ml H_2O and tissues were removed with a Waterpik Ultra Water Flosser. Skeletons were rinsed in ultrapure water and dried at room temperature.

To determine if fluorescent beads could pass through the cell layers, microcolonies grown on glass coverslips were incubated for 20 min in 5 ml fSW-containing 2 per cent fluorescent beads (each size independently) under mixing with a magnetic stirrer. Observations were performed with the confocal microscope (see below).

(e) *Observations of samples (calcein and fluorescent beads)*
As specified for each experiment, observations were made either with a fluorescent macroscope (Z16APO, Leica Microsystems) or with an inverted confocal laser-scanning microscope (TCS SP5, DMI 6000 CS, Leica Microsystems).

Quantitative measurements of calcein were obtained with the confocal system by spectral analysis with excitation at 488 nm.

For calcein and fluorescent beads observed with the Leica Z16APO macroscope or the Leica DMI 6000 CS microscope, samples were excited, respectively, with blue and green light, and emission fluorescence was detected using a JVC 3CCD digital camera.

For fluorescence spectra of calcein in confocal microscopy, measurements were made with a spectrofluorimeter coupled to the imaging system with 488 nm laser excitation.

For confocal images of calcein, excitation wavelength was 488 nm and emission was 515 ± 15 nm. For confocal images
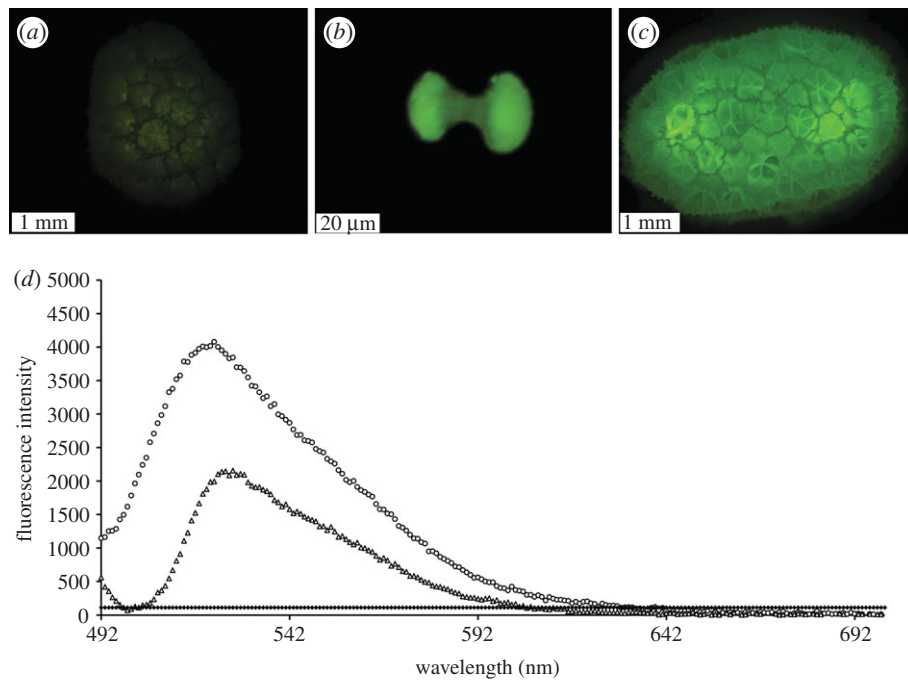
Figure 1. (*a–c*) Observation of coral skeletons and calcium carbonate crystal with a fluorescent macroscope (blue light excitation). (*a*) Faint yellow–green autofluorescence of a coral bare skeleton (without preliminary incubation with calcein). (*b*) Green fluorescence of an inorganic calcium carbonate crystal aggregate precipitated in the presence of calcein. (*c*) Green fluorescence of a coral skeleton observed after incubation of a live microcolony with calcein and removal of tissues. (*d*) Emission spectra obtained with a spectrofluorimeter coupled to a confocal microscope (excitation = 488 nm). Autofluorescence of a coral bare skeleton (black line), fluorescence of a skeleton after incubation of live coral microcolony with calcein (circles), and fluorescence of calcein in sea water at pH 8.2 (triangles).

of red fluorescent beads, excitation wavelength was 543 nm and emission was 605 ± 15 nm.

(f) Electrophysiological experiments
(i) Preparation of samples
Microcolonies of the coral *S. pistillata* were cultured over perforated glass slides with a hole of 2.5 mm radius and 0.2 cm^2 surface area, on which the apex of the coral was placed (for details of the experimental set-up, see electronic supplementary material, figure S1*a–d* and material and methods). The sea anemone, *A. viridis*, was also used since this anthozoan possesses long tentacles from which oral tissues are easy to obtain. Briefly, one piece of tentacle was cut longitudinally and placed between the two Ussing half-chambers as described previously by Bénazet-Tambutté *et al.* [31]. Resistance was then calculated from the values of intensity and voltage (for details see electronic supplementary material, material and methods).

3. RESULTS
(a) Calcein, calcium carbonate and fluorescence
To determine the potential autofluorescence of the samples, we observed a bare coral skeleton under excitation with blue light. As can be seen in figure 1*a*, the control bare coral skeleton (without calcein) shows a faint yellow–green autofluorescence. This signal is weaker than the bright green fluorescence owing to the incorporation of calcein (i) in calcium carbonate crystals precipitated *in vitro* (figure 1*b*) and (ii) in the skeleton of live microcolonies during *in vivo* experiments (figure 1*c*). The spectral analysis showed that calcein incorporated into coral skeleton of live microcolonies gives an emission spectrum (after excitation at 488 nm) similar to calcein in

sea water, whereas the control bare coral (without calcein) gives negligible emission under excitation at 488 nm (figure 1*d*). Spectra obtained after dissolution of skeletons from live microcolonies incubated with calcein had identical spectra to those obtained for calcein in sea water treated with HCl and NaOH (final pH 8.2; data not shown).

(b) Calcein incorporation into coral skeleton
The following observations were obtained with a macroscope but results were always checked by spectral analysis in order to discriminate between autofluorescence and fluorescence owing to calcein (as described above). Figure 2*a,b,c* respectively, show the fluorescence of (i) the skeleton from a live microcolony (microcolony = skeleton + tissue), (ii) a bare skeleton (=skeleton without tissues) and (iii) the skeleton from a dead microcolony (dead microcolony = microcolony killed with NaCN, 1 mM, 2 h, = skeleton with dead tissues), all after incubation in calcein. Except for the bare skeleton, the incubations were performed in the presence of tissues. Further treatment of the skeletons with NaOCl revealed that calcein labelling is removed (labile) in bare skeletons and skeletons from dead microcolonies, indicating that it is adhering superficially to the CaCO$_3$ (results not shown). By contrast, in live microcolonies, calcein is permanently incorporated into the skeletons as a result of calcification. In live corals, calcein is incorporated into the newly forming crystals in areas such as septa and columella of corallites (figure 2*d*), individual granules of calcium carbonate growing on glass slides (figure 2*e*) and forming spines (figure 2*f*). Complementary experiments to show that the green granules in figure 2*e* are due to the incorporation of calcein in calcium carbonate granules
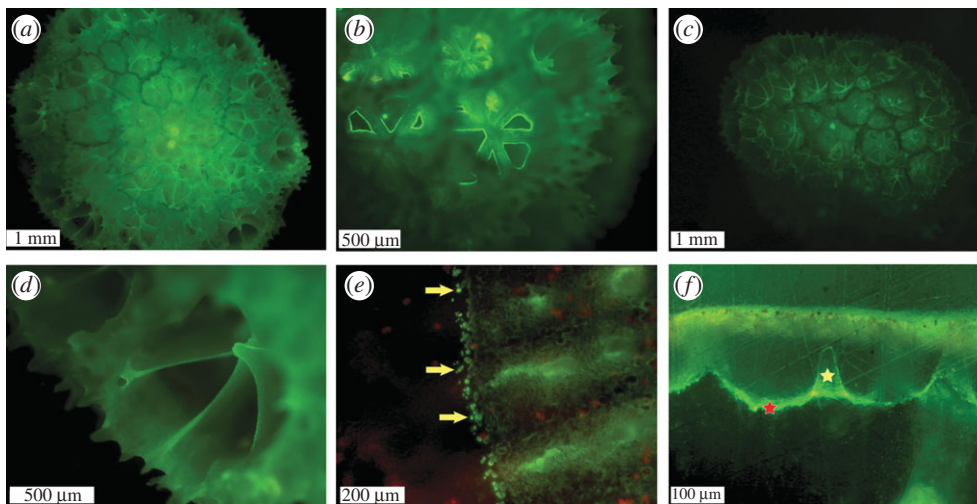
Figure 2. Observation of calcein incorporation into coral skeleton with a fluorescent macroscope (blue light excitation; fluorescence emission is in green). (*a*) Bright fluorescence of the skeleton of a live microcolony incubated with calcein. (*b*) Fluorescence of a bare skeleton incubated with calcein. (*c*) Fluorescence of the skeleton of a dead microcolony incubated with calcein. (*d*) Fluorescent labelling of the septa and columella of a corallite (magnification of (*a*)). (*e*) Fluorescence of calcein incorporated in newly forming crystals of calcium carbonate (yellow arrows) in a live microcolony growing on a glass slide (observed upside-down, 7 days after calcein labelling). (*f*) Fluorescent labelling in the coenosteum (red star) and the spines (yellow star) in section of a live microcolony incubated with calcein and embedded in resin. All samples were incubated for 20 min in fSW-calcein 20 µM.

and not to green fluorescent proteins (GFP) are presented as the electronic supplementary material, figure S2*a*–*f*. All these results show that, while calcein may superficially bind to a bare skeleton or a skeleton from a dead microcolony, it is permanently incorporated (resistant to NaOCl treatment) into calcifying zones of live growing corals.

(c) Stoichiometry of calcein incorporation into the skeleton

The amount of calcein incorporated into the skeletons of live microcolonies was estimated using the calibration curve of calcein as described in §2. The results were obtained as a function of time (2, 4, 6 and 24 h). The rate of calcein incorporation has a value of 0.08 nmol calcein g^{-1} dry skeleton h^{-1}. In parallel, the rate of calcification was measured by the alkalinity anomaly technique and has a value of 3302 ± 173 nmol $CaCO_3$ g^{-1} dry skeleton h^{-1}. The equation of the slopes fitted with linear regression was $y = 3344.8x$ for alkalinity and $y = 0.0771x$ for calcein. Equality of the slopes was tested on normalized values (normalization by the mean, $n = 5$ samples) using GraphPad Prism (v. 5.0), which confirmed that they were not statistically different (ANCOVA, $p = 0.40$, $F = 0.82$). The results are presented in figure 3 as the rate of calcein incorporation versus the rate of calcification. In our experimental conditions, the rate of calcein incorporation is far lower than the rate of calcium incorporation (ratio of 2×10^{-5}).

(d) Paracellular versus transcellular pathway of calcein

We investigated the permeability of coral tissues to calcein (which is known to be impermeant to cells owing to its hydrophilic properties) by observing whole tissues of microcolonies grown on glass coverslips (for histology, see [28]) and incubated with calcein (figure 4). Using an inverted confocal microscope, we could focus on
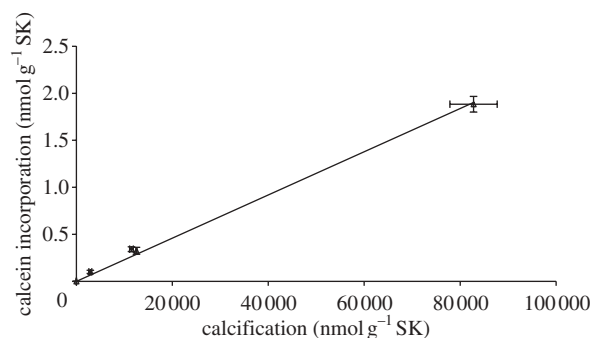

Figure 3. Calcein incorporation as a function of calcification in microcolonies incubated for different time periods with calcein 20 µM. Calcification rates were measured with the alkalinity anomaly technique and are expressed in nmol $CaCO_3$ g^{-1} dry skeleton. Incorporation of calcein in skeletons was determined by measuring the intensity of fluorescence (confocal laser-scanning microscope) after dissolution of skeletons and by reporting this value of intensity on the calcein calibration curve. Results are presented as means + s.d.; $n = 5$ samples.

specific optical sections obtained by z-stack analysis through the preparation from tissues and growing crystals in contact with the coverslip to the upper tissues. As can be seen in figure 4*b*, calcein is present in the outside medium but also between oral ectodermal cells. Control experiments without calcein (figure 4*a*) allow us to determine that intracellular small green fluorescent dots are due to autofluorescent proteins. The same paracellular distribution of calcein was also observed in the endodermal tissues (figure 4*d*). We could also observe the tissue directly in contact with the coverslip and surrounding the growing crystals (i.e. the calicoblastic ectoderm). In control experiments without calcein, there was no fluorescence owing to autofluorescent proteins in the calicoblastic ectoderm. We had to use a higher concentration of calcein (160 µM) because the calicoblastic cells are very thin and labelling was difficult to observe. As can
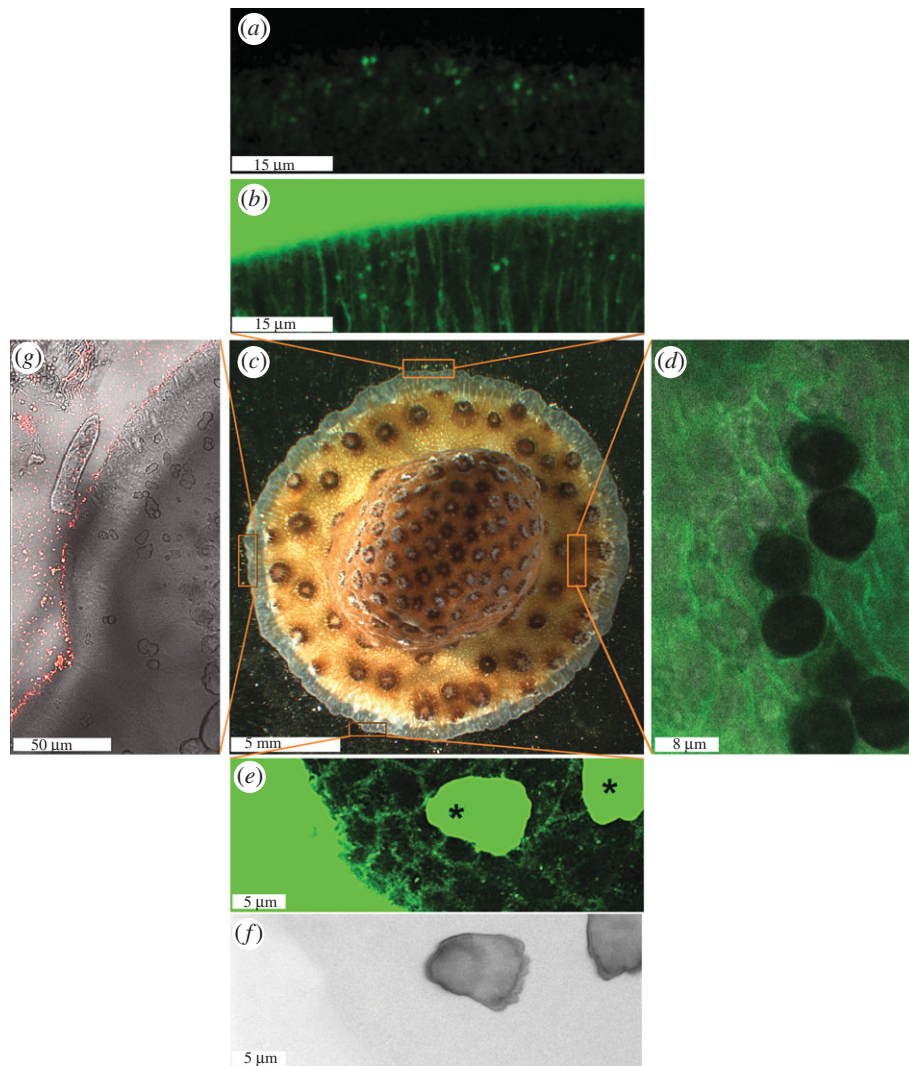
Figure 4. Characterization of the paracellular pathway. (*a*–*f*) Experiments with microcolonies grown on glass coverslips. Except for (*c*), observations were made with the inverted microscope of a confocal and the z-stack tool was used to position the observation. (*c*) Representative microcolony grown on a glass coverslip and observed with bright field light, observation with a macroscope. (*a*) Control microcolony without any incubation, magnification of the upper zone of (*c*). Small green autofluorescent dots are due to autofluorescent proteins. (*b*) Microcolony incubated for 20 min in the presence of calcein 20 μM, magnification of the upper zone of (*c*). Small green fluorescent dots are due to autofluorescent proteins whereas paracellular green fluorescence in oral ectoderm is due to calcein. (*d*) Microcolony incubated for 20 min in the presence of calcein 20 μM, magnification of the right zone of (*c*). Paracellular green fluorescence of endodermal cells is due to calcein; the image is merged with a bright field transmitted light image in which zooxanthellae appear as black spheres (the optical section is 17 μm above the coverslip, taken from a z-stack with a 0.3 μm step). (*e*) Microcolony incubated for 20 min in the presence of calcein 160 μM, magnification of the lower zone of (*c*). Paracellular green fluorescence in calicoblastic ectoderm surrounding the two fluorescent crystals (asterisks) is due to calcein (the optical section is 1 μm above the coverslip). (*f*) Bright field transmitted light allows confirming that the two large fluorescent zones in (*e*) are due to calcein incorporated into calcium carbonate crystals (arranged as fasciculi). (*g*) Microcolony incubated for 20 min with 200 nm red fluorescent beads, magnification of the left zone of (*c*). The image is a merging of bright field transmitted light and red fluorescence. Crystals can be distinguished in the growing front and are surrounded by tissues whereas red fluorescent beads remain outside the tissues.

be seen in figure 4*e*, calcein is present between the calicoblastic cells, and the two green high fluorescent zones (asterisks) are due to calcein incorporated into forming crystals (crystals arranged as fasciculi can be seen with bright field transmitted light; figure 4*f*).

(e) Permeability of the tissues to fluorescent beads
To estimate the size of the paracellular pathway, we incubated microcolonies with fluorescent beads of different sizes (20 nm, 200 nm or 2 μm), removed the tissues and observed the skeleton. We did not observe any labelling of the skeleton whatever the size of the fluorescent beads

(observations performed with a fluorescent macroscope and microscope; results not shown since no fluorescence was observed). We confirmed this result by incubating the microcolonies grown on coverslips with the fluorescent beads of different sizes. In this case, we looked at the tissues with the confocal microscope (inverted microscope) using both bright field transmitted light and fluorescence, and the z-stack tool. As can be seen in figure 4*g* for the 200 nm diameter beads, regardless of their size, the red fluorescent beads remained at the periphery of the tissues and were never found either in the tissues or in the new growing calcium carbonate crystals, thus confirming that the tissues are not permeable to molecules of 20 nm diameter or more.

(f) Determination of tissues and skeleton resistance

Voltage-clamp experiments in Ussing chambers were performed to determine the electrical resistance of the tissues of *S. pistillata*. We found a value of 1483 ± 189 Ohm cm^2 for the resistance of whole microcolonies (tissues covering the skeleton). We then removed the tissues and found a value of 1006 ± 175 Ohm cm^2 for the resistance of the bare skeleton. By subtracting the resistance of the bare skeleton from the resistance of the whole microcolony, we obtained a value of 477 ± 21 Ohm cm^2 for the resistance of the tissues (oral and aboral tissues). Since it was impossible to separate the oral tissue from the aboral tissue in *S. pistillata*, we measured the resistance of the oral tissue of the sea anemone *A. viridis* and obtained a value of 15 ± 3 Ohm cm^2. We then performed a hyperosmotic shock, which is usually used to determine if junctions are involved in the paracellular resistance of tissues [32]. When the hyperosmotic shock was performed in the hemi-chamber facing the tissues (apex) of a microcolony, the resistance decreased as a function of time (electronic supplementary material, figure S3). Since there was no decrease in the resistance of a bare skeleton under hyperosmotic shock (results not shown), we can confirm that we really measured the resistance of the tissues and we can conclude that, under hyperosmotic shock, the tissues became less resistant to electric current.

4. DISCUSSION

(a) Calcein incorporation and coral calcification rate

In corals and in other calcifying organisms, calcein is widely used to indicate skeletal growth. Indeed organisms exposed to this fluorochrome incorporate it into growing calcified structures in the form of an internal growth mark (observable under excitation with fluorescent blue light) that can subsequently be used to estimate growth from time of exposure. We first compared the spectrum of the fluorescent signal obtained from corals labelled with calcein with the autofluorescence signal of the calcium carbonate of coral skeletons. Clearly, the spectra were different (figure 1). Then, we showed that calcein is incorporated (i) into calcium carbonate crystals precipitated inorganically and (ii) in newly formed crystals present in calcifying zones of coral skeleton, such as spines, septa or columella. We observed that the labelling of bare skeletons or dead microcolonies was labile (after treatment with NaOCl), whereas it was stable in similarly treated skeletons in live microcolonies. In parallel to calcein incorporation, we measured the calcification rate by the alkalinity anomaly technique. In our experimental conditions, we showed that calcein incorporation is proportional to calcification with a molar ratio of 2×10^{-5}. We can thus conclude that calcein may be a useful tool for estimating coral calcification rates. Such a result was also obtained (i) in the coral *Pocillopora damicornis* with incorporation of the dye alizarin red S (which showed a high correlation with calcium incorporation [33]), and (ii) in osteoblasts in culture with incorporation of calcein as a semi-quantitative measurement of mineralization of calcium phosphate [34].

(b) Insight on transepithelial transport from experiments with fluorescent molecules

Evidence supporting the transport of bulk sea water to the site of calcification includes observations that molecules such as calcein or alizarin are rapidly incorporated from the surrounding sea water into coral skeleton. However, the pathway of these molecules through the tissues has never been characterized in corals nor in other calcifying organisms.

Our data allow us to conclude that the hydrophilic molecule calcein is transported via a paracellular pathway at the level of the coral tissue layers, including the calicoblastic ectoderm. Indeed, we have shown (i) that calcein is incorporated into the skeleton, indicating that it crosses the four cell layers (unless it is coming from the sea water present in the coelenteron, and then it crosses only two layers); and (ii) that calcein cannot enter into cells, suggesting that it has to pass through a paracellular pathway through the four (or two) cell layers. Using confocal microscopy, we visualized the paracellular pathway with images of calcein between cells of the oral ectoderm and calicoblastic ectoderm (and observed that this was also the case for endoderms). We have shown that fluorescent beads of different sizes were not incorporated into the skeleton and that they were not present between cells. This finding supports the idea that (i) calcein passes through intercellular spaces, such as described in different coral species [7,21,22], and (ii) there are no holes in the tissue through which molecules can pass (holes in the tissues have only been evidenced by microscopy observations in the oral tissues [35,36], never in the calicoblastic ectoderm).

In vertebrates, the gatekeeper of the paracellular pathway is the tight junction, which is an apically located cell–cell interaction of epithelial cells. This tight junction allows the selective pathway of ions while restricting the movement of large molecules. Permeability studies using membrane impermeant tracers suggest that the tight junction has pores of approximately 6–7 Å diameter [37]. In the case of corals, based on ultrastructural studies, the septate junction has been considered the counterpart of the mammalian tight junction and has been localized in the calicoblastic cell layer [7,21,22] (electronic supplementary material, figure S4). Since calcein passes through a paracellular pathway, it has to diffuse through these junctions. We can thus conclude that the septate junctions should possess pores of a larger size than the tight junction (at least twice the size of the molecular radius of calcein, i.e. 13 Å [38]). However, since fluorescent beads of 20 nm do not pass through the epithelial layers, we can conclude that the size of the septate junctions is less than 20 nm. Therefore, combined with the results on calcein, we can conclude that, in corals, the septate junctions present in the paracellular pathway should possess pores of more than 13 Å and less than 20 nm.

(c) Insight on epithelial permeability from electrophysiology experiments

Transepithelial transport of ions/molecules by a paracellular pathway is dependent not only on the size but also on the charge of ions/molecules [39]. The technique of electrophysiology with Ussing chambers has been used for many years to estimate the 'tightness' versus the 'leakiness' of the epithelial layers. Indeed, voltage clamp experiments indicate whether an epithelial layer forms a low- or high-resistance barrier to ion diffusion and give insight into the importance of the paracellular versus the

transcellular pathway. In leaky epithelia, resistance values are classically between 6 and 100 Ohm cm^2, whereas in tight epithelia, these values range from 500 to 70 000 Ohm cm^2 [40,41]. In the present study, electrophysiology experiments show that the tissues have a resistance of 477 ± 42 Ohm cm^2. This value could be considered 'intermediate', but it is located closer to the lower range of values for mammalian tight epithelia (for comparative values, see electronic supplementary material, table S1). Moreover, this resistance is very high when compared with the resistance of the oral tissue of sea anemones (present study and [31]). Electrophysiology experiments cannot be done on the coral oral tissue owing to technical limitations, but structural similarities between coral and anemone oral tissues [42] suggest that results should be comparable, and if this was the case the higher resistance of the tissues of *S. pistillata* would be due to the paracellular junctions of the aboral tissue. In epithelia, permeability due to the paracellular pathway is known to increase under hyperosmotic conditions with non-electrolyte solutions by opening junctions [32,43]. In this study, we have observed that a hyperosmotic shock leads to a decrease in microcolony resistance, and thus an increase in tissue permeability. In mammals, electronic microscopic observations show changes in the geometry of junctional complexes compatible with an increase in permeability during hyperosmotic shock [43] causing the opening of septate junctions [44]. The effect of hyperosmotic shock by decreasing coral tissue resistance supports the interpretation that in normal conditions (without osmotic shock), paracellular junctions control and restrict the diffusion of molecules, and thus play a key role in determining the permeability properties of the epithelial layers.

(d) Epithelial permeability and ion transport in corals and other organisms

From the results obtained in the present study on the permeability of tissues to calcein, it is tempting to widen the discussion to ions involved in the calcification process, such as calcium. A direct comparison between calcium incorporation and calcein incorporation in the coral skeleton is not possible for the moment since there is no data in the literature for how calcein is incorporated into calcium carbonate. It is, however, possible to consider our results in context with the existing literature on calcium transport, both in corals and other systems. Studies aimed at determining the mechanisms of calcium transport across coral tissues have shown that, at the level of the oral tissues, calcium is transported either by an active transcellular pathway [21,45] or by a passive paracellular pathway [12,31]. Moreover, at the level of the calicoblastic ectoderm, data suggest that the transport of calcium for calcification is active and transcellular [10−14], and it has been shown that there is an increasing intracellular gradient of calcium from the oral cells facing external sea water to the calicoblastic layer of the aboral tissue [46]. Since the size of calcium ions (atomic radius of calcium is 1.8 Å) is far lower than the size of calcein (molecular radius of calcein is 6.5 Å), it is not possible to rule out the possibility that in addition to the transcellular pathway mentioned above, there is also a paracellular pathway of calcium. However, since the
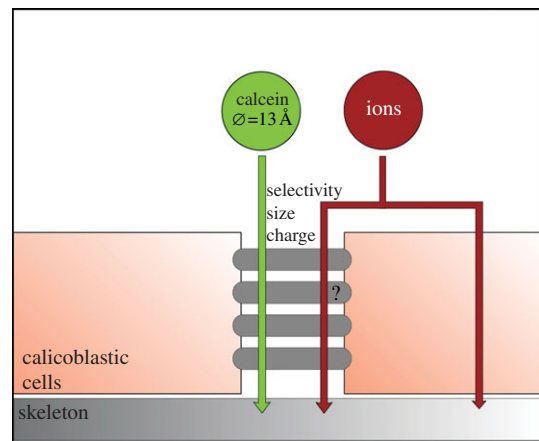

Figure 5. Schematic of the transfer of calcein and the possible transfer of ions in the calicoblastic cell layer. The paracellular pathway through the junctions is dependent on the size and charge of molecules and ions. For calcein, the pathway is derived from the present study, whereas for ions (and especially calcium) it is also derived from the literature (see text for references), and the relative contribution of the paracellular and transcellular transport mechanisms to the overall calcium transport remains unknown.

paracellular pathway also depends on the charge of ions/molecules (calcium is positively charged and calcein is negatively charged at pH 8.2), the relative contribution of the paracellular and transcellular transport mechanisms to the overall calcium transport remains unknown. Looking at vertebrate systems in which calcium transport is better characterized (e.g. in the mammalian intestine), it appears that even in tight epithelia both paracellular and transcellular modes of transport are possible, with a percentage of each depending on the epithelium properties and physiological conditions (see table 1 in [47]). In invertebrates, as mentioned in §1, the counterpart of the tight junction is the septate junction, which has been evidenced in corals only by ultrastructural studies, and this septate junction is presented as serving as a paracellular barrier to diffusion [23]. However, if we look at the transport of calcium by the shell epithelium of the freshwater clam *Anodonta cygnea*, it appears that a transcellular calcium transport coexists with paracellular diffusion through septate junctions [24]. In the present study, we have shown by electrophysiology experiments combined with confocal microscopy that even if calcein can pass through a paracellular pathway, the paracellular junctions control and restrict the diffusion of molecules (osmotic shock experiment), and thus play a key role in determining the permeability properties of the epithelial layers. Until now no molecular characterization of junctions has ever been performed in corals, but such studies will be necessary in the future to characterize the structural elements, which are central to establishing an effective paracellular diffusion barrier to ions and molecules.

5. CONCLUSION

The results of the present study show that, in corals, calcein enters the calcification environment via a paracellular pathway with paracellular junctions controlling and restricting the diffusion of molecules. From these data, we propose a schematic of the transfer of calcein and the possible transfer of ions at the level of calicoblastic cells (figure 5). From our

results, we draw attention to some crucial points that need to be taken into account: (i) the role of paracellular junctions in ions/molecules transport; (ii) the significance of the value of the epithelial resistance owing to paracellular junctions; and (iii) the usefulness of studying molecules such as calcein for characterizing epithelial properties (but also the necessary precaution when extrapolating results for other ions such as calcium). Whereas our results suggest at least semi-open exchange with the surrounding sea water, both transcellular and paracellular processes for ion transport need to be explored through future research.

REFERENCES

1 Allemand, D., Ferrier-Pagès, C., Furla, P., Houlbrèque, F., Puverel, S., Reynaud, S., Tambutté, É., Tambutté, S. & Zoccola, D. 2004 Biomineralisation in reef-building corals: from molecular mechanisms to environmental control. *C. R. Paleoevol.* **3**, 453–467. (doi:10.1016/j.crpv.2004.07.011)

2 Barnes, D. J. & Chalker, B. E. 1990 Calcification and photosynthesis in reef-building corals and algae. In *Coral Reefs* (ed. Z. Dubinsky), pp. 109–131. Amsterdam, The Netherlands: Elsevier.

3 Buddemeier, R. W. & Kinzie, R. A. 1976 Coral growth. *Oceanogr. Mar. Biol. Annu. Rev.* **14**, 183–225.

4 Cohen, A. L. & McConnaughey, T. A. 2003 A geochemical perspective on coral mineralization. In *Biomineralization, Rev Mineral Geochem*, vol. 54 (eds P. M. Dove, J. J. De Yoreo & S. Weiner), pp. 151–187. Washington, DC: Mineralogical Society of America.

5 Constantz, B. R. 1986 Coral skeleton construction: a physiochemically dominated process. *Palaios* **1**, 152–157. (doi:10.2307/3514508)

6 Gattuso, J.-P., Allemand, D. & Frankignoulle, M. 1999 Photosynthesis and calcification at cellular, organismal and community levels in coral reefs: a review on interactions and control by carbonate chemistry. *Am. Zool.* **39**, 160–183.

7 Johnston, I. S. 1980 The ultrastructure of skeletogenesis in zooxanthellate corals. *Int. Rev. Cytol.* **67**, 171–214. (doi:10.1016/S0074-7696(08)62429-8)

8 Muscatine, L. 1971 Calcification in corals. In *Experimental coelenterate biology* (eds H. M. Lenhoff, L. Muscatine & L. V. Davis), pp. 227–237. Honolulu, HI: University Press of Hawaii.

9 Allemand, D., Tambutté, É, Zoccola, D. & Tambutté, S. 2011 Coral calcification, cells to reefs. In *Coral reefs: an ecosystem in transition* (eds Z. Dubinsky & N. Stambler), part III, pp. 119–150. Berlin, Germany: Springer.

10 Chalker, B. E. 1976 Calcium transport during skeletogenesis in hermatypic corals. *Comp. Biochem. Physiol.* **54 A**, 455–459. (doi:10.1016/0300-9629(76)90049-9)

11 Marshall, A. T. 1996 Calcification in hermatypic and ahermatypic corals. *Science* **271**, 637–639. (doi:10.1126/science.271.5249.637)

12 Tambutté, É., Allemand, D., Mueller, E. & Jaubert, J. 1996 A compartmental approach to the mechanism of calcification in hermatypic corals. *J. Exp. Biol.* **199**, 1029–1041.

13 Zoccola, D., Tambutté, É., Sénegas-Balas, F., Michiels, J.-F., Failla, J.-P., Jaubert, J. & Allemand, D. 1999 Cloning of a calcium channel alpha-1 subunit from the reef-building coral, *Stylophora pistillata*. *Gene* **227**, 157–167. (doi:10.1016/S0378-1119(98)00602-7)

14 Zoccola, D., Tambutté, É., Kulhanek, E., Puverel, S., Scimeca, J. C., Allemand, D. & Tambutté, S. 2004 Molecular cloning and localization of a PMCA P-type calcium ATPase from the coral *Stylophora pistillata*. *Biochim. Biophys. Acta* **1663**, 117–126. (doi:10.1016/j.bbamem.2004.02.010)

15 Braun, A. & Erez, J. 2004. Preliminary observations on sea water utilization during calcification in scleractinian corals. In *American Geophysical Union Fall Meeting, San Francisco, 13–17 December*, Abstract no. B14B-04, see http://adsabs.harvard.edu/abs/2004AGUFM.B14B. 04B (accessed 2 December 2009).

16 Cohen, A. L., McCorkle, D. C., De Putron, S., Gaetani, G. A. & Rose, K. A. 2009 Morphological and compositional changes in the skeletons of new coral recruits reared in acidified seawater: insights into the biomineralization response to ocean acidification. *Geochem. Geophys. Geosyst.* **10**, 1–12. (doi:10.1029/2009GC 002411)

17 Erez, J., Schneider, K., Silverman, J., Braun, A., Bentov Mor Grinstein, S. & Lazar, B. 2005 *Biomineralization of $CaCO_3$ in the oceans: a major negative feedback mechanism to atmospheric CO_2 increase*. Abstracts of the 9th Biomineralization Symp. Pucon, Chile 2005.

18 Erez, J. & Braun, A. 2007 Calcification in hermatypic corals is based on direct seawater supply to the biomineralization site, 17th Annual V M Goldschmidt, Cologne, Germany. *Geochim. Cosmochim. Acta* **71**, A260–A260.

19 Barnes, D. J. 1970 Coral skeletons: an explanation of their growth and structure. *Science* **170**, 1305–1308. (doi:10.1126/science.170.3964.1305)

20 Barnes, D. J. 1972 The structure and formation of growth-ridges in scleractinian coral skeletons. *Proc. R. Soc. Lond. B* **182**, 331–350. (doi:10.1098/rspb.1972.0083)

21 Clode, P. L. & Marshall, A. T. 2002 Low temperature FESEM of the calcifying interface of a scleractinian coral. *Tissue Cell* **34**, 187–198. (doi:10.1016/S0040-8166(02)00031-9)

22 Tambutté, É., Allemand, D., Zoccola, D., Meibom, A., Lotto, S., Caminiti, N. & Tambutté, S. 2007 Observations of the tissue–skeleton interface in the scleractinian coral *Stylophora pistillata*. *Coral Reefs* **26**, 517–529. (doi:10.1007/s00338-007-0263-5)

23 Faivre-Sarrailh, C., Banerjee, S., Li, J., Hortsch, M., Laval, M. & Bhat, M. A. 2004 *Drosophila* contactin, a homolog of vertebrate contactin, is required for septate junction organization and paracellular barrier function. *Development* **131**, 4931–4942. (doi:10.1242/dev.01372)

24 Bleher, R. & Machado, J. 2004 Paracellular pathway in the shell epithelium of *Anodonta cygnea*. *J. Exp. Zool.* **301A**, 419–427. (doi:10.1002/jez.a.20065)

25 Tambutté, É., Allemand, D., Bourge, I., Gattuso, J.-P. & Jaubert, J. 1995 An improved ^{45}Ca protocol for investigating physiological mechanisms in coral calcification. *Mar. Biol.* **122**, 453–459. (doi:10.1007/BF00350879)

26 Muscatine, L., Tambutté, É. & Allemand, D. 1997 Morphology of coral desmocytes, cells that anchor the calicoblastic epithelium to the skeleton. *Coral Reefs* **16**, 205–213. (doi:10.1007/s003380050075)

27 Reynaud-Vaganay, S., Gattuso, J. P., Cuif, J.-P., Jaubert, J. & Juillet-Leclerc, A. 1999 A novel culture technique for scleractinian corals: application to investigate changes in skeletal ∂^{18}O as a function of temperature. *Mar. Ecol. Prog. Ser.* **180**, 121–130. (doi:10.3354/meps180121)

28 Raz-Bahat, M., Erez, J. & Rinkevich, B. 2006 *In vivo* light-microscopic documentation for primary calcification processes in the hermatypic coral *Stylophora pistillata*. *Cell Tissue Res.* **325**, 361–368. (doi:10.1007/s00441-006-0182-8)

29 Moran, A. L. 2000 Calcein as a marker in experimental studies newly-hatched gastropods. *Mar. Biol.* **137**, 893–898. (doi:10.1007/s002270000390)

30 Smith, S. V. & Key, G. S. 1975 Carbon dioxide and metabolism in marine environment. *Limnol. Oceanogr.* **20**, 493–495. (doi:10.4319/lo.1975.20.3.0493)

31 Bénazet-Tambutté, S., Allemand, D. & Jaubert, J. 1996 Permeability of the oral epithelial layers in cnidarians. *Mar. Biol.* **126**, 43–53. (doi:10.1007/BF00571376)

32 Nilsson, H., Dragomir, A., Ahlander, A., Johannesson, M. & Roomans, G. M. 2007 Effects of hyperosmotic stress on cultured airway epithelial cells. *Cell Tissue Res.* **330**, 257–269. (doi:10.1007/s00441-007-0482-7)

33 Lamberts, A. E. 1974 Measurement of alizarin deposited by corals. In *Proc. Second Int. Coral Reef Symp.* pp. 241–244. Brisbane, Australia: Great Barrier Reef Committee.

34 Hale, L. V., Ma, Y. F. & Santerre, R. F. 2000 Semi-quantitative fluorescence analysis of calcein binding as a measurement of *in vitro* mineralization. *Calcif. Tissue Int.* **67**, 80–84. (doi:10.1007/s00223001101)

35 Schlichter, D. 1991 A perforated gastrovascular cavity in the symbiotic deep-water coral *Leptoseris fragilis*: a new strategy to improve heterotrophic nutrition in corals. *Helgoländer Meeresuntersuchungen* **45**, 423–443. (doi:10.1007/BF02367177)

36 Fautin, D. G. & Mariscal, R. N. 1991 Cnidaria: Anthozoa. In *Placozoa, Porifera, Cnidaria, and Ctenophora*, vol. 2 (eds F. W. Harrison & J. A. Westfall), pp. 267–358. New York, NY: Wiley-Liss.

37 Tang, V. W. & Goodenough, D. A. 2003 Paracellular ion channel at the tight junction. *Biophys. J.* **84**, 1660–1673. (doi:10.1016/S0006-3495(03)74975-3)

38 McAllister, D., Wang, P., Davis, S., Park, J., Canatella, P., Allen, M. & Prausnitz, M. 2003 Microfabricated needles for transdermal delivery of macromolecules and nanoparticles: fabrication methods and transport studies. *Proc. Natl Acad. Sci. USA* **100**, 13 755–13 760. (doi:10.1073/pnas.2331316100)

39 Powell, D. W. 1981 Barrier function of epithelia. *Am. J. Physiol.* **241**, G275–G288.

40 Frömter, E. & Diamond, J. 1972 Route of passive ion permeation in epithelia. *Nat. New Biol.* **235**, 9–13. (doi:10.1038/235009a0)

41 Lewis, S. A. 1996 Epithelial structure and function. In *Epithelial transport: a guide to methods and experimental analysis* (eds N. K. Wills, L. Reuss & S. A. Lewis), pp. 1–20. London, UK: Chapman and Hall.

42 Allemand, D., Furla, P. & Bénazet-Tambutté, S. 1998 Mechanisms of carbon acquisition for endosymbiont photosynthesis in Anthozoa. *Can. J. Bot.* **76**, 925–941.

43 Fowler, N., Gonzalez, E., Rawlins, F. A., Giebisch, G. H. & Whittemburry, G. 1977 Effect of hypertronic urea and mannitol on distal nephron permeability. *Pflugers Arch.* **368**, 3–11. (doi:10.1007/BF01063448)

44 Dan-Sohkawa, M., Kaneko, H. & Noda, K. 1995 Paracellular, transepithelial permeation of macromolecules in the body wall epithelium of starfish embryos. *J. Exp. Zool.* **271**, 264–272. (doi:10.1002/jez.1402710404)

45 Wright, O. P. & Marshall, A. T. 1991 Calcium transport across the isolated oral epithelium of scleractinian corals. *Coral Reefs* **10**, 37–40. (doi:10.1007/BF00301905)

46 Marshall, A. T., Clode, P. L., Russell, R., Prince, K. & Stern, R. 2007 Electron and ion microphobe analysis of calcium distribution and transport in coral tissues. *J. Exp. Biol.* **210**, 2453–2463. (doi:10.1242/jeb.003343)

47 Khanal, R. C. & Nemere, I. 2008 Regulation of intestinal calcium transport. *Annu. Rev. Nutr.* **28**, 179–196. (doi:10.1146/annurev.nutr.010308.161202)